Nonlinear dynamic analysis of non-ideal motor foundations

Henrique Z. D. S. Vieira[1], Carlos E. N. Mazzilli[1],

[1]*Dept. of Structural and Geotechnical Engineering, Escola Politécnica of the University of São Paulo*
Av. Prof. Almeida Prado 83, 05508-070, São Paulo, Brazil
henriquezarnauskas@usp.br, cenmazzi@usp.br

Abstract. This paper addresses the electromechanical coupled response of interconnected foundations of non-ideal motors, identifying the relevant parameters for the phenomenon of machine synchronization. DC electric motors are considered in the model, using a linear approximation of the characteristic curve (angular velocity x torque), delineating the electromechanical coupling. To obtain the 2D projections of the basins of attractions of stable solutions, the $(\psi_2 - \psi_1)$ x $(\psi_2' - \psi_1')$ plane was chosen at different voltages. These planes were divided into several square cells and, for each one of them being obtained the self-synchronization attractor. To obtain the projections of the basins of attraction, the electrical voltage was kept constant over time.

It was identified that synchronizations occur for unbalanced rotors angle differences of zero or π radians. It was observed that there is a gradual change of attractors between dimensionless voltages 0.66 and 0.74 (6.70 V and 7.50 V), in addition to another change of attractors between dimensionless voltages 1.25 and 1.39 (12.7 V and 14.5 V).

Keywords: Attractors, Self-synchronization, Basins of attraction, Non-linear vibrations, Non-ideal motors.

1 Introduction

The object of this research is to study the self-synchronization of non-ideal motors supported on separate foundations elastically connected, continuing the studies done in [1], identifying the relevance of motor voltage for this phenomenon and the types of synchronization of the machines, studying the basins of attraction.

2 Torque of electric motors

In this article, non-ideal motors are considered and their synchronization observed. DC electric motors will be addressed in the model for the sake of an illustration.

Kononenko [2] studied the characteristic curves of the motors and the Somerfeld effect [3] of motors supported by a cantilever. Say and Taylor [4] studied the steady-state operating point of the engines. Lobosto and Dias [5] deepened these studies, commenting that the characteristic curve of the engines present a decrease in torque for increasing angular velocity. In the present research, an approximation of the characteristic curve of parallel DC motors will be used (see Fig. 1 and Fig. 2).

To obtain the approximate characteristic curve function, the control equation shown below will be used.

$$u - e_{cemf} = R_a i_a + L_a \dot{i}_a \tag{1}$$

The counter-electromotive force can be expressed in proportion to the angular velocity of the motor ($e_{cemf} = k_E \dot{\psi}$), just as the motor torque can be expressed in proportion to the electrical current of the circuit ($M_i = k_M i_a$). In this way eq. (2) can be written:
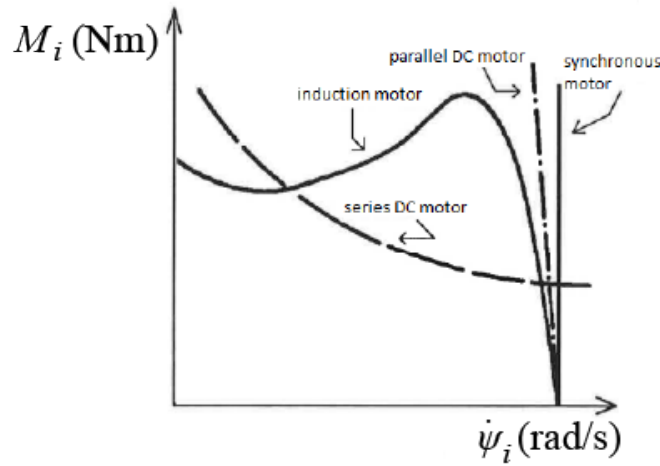
Figure 1. Characteristic curves of the motors: Adapted from Lobosco, O. S., and Dias, J., 1988

$$u - k_E \dot{\psi}_i = \frac{R_a}{k_M} M_i + \frac{L_a}{k_M} \dot{M}_i \qquad (2)$$

In a stable regime, for which $\dot{M}_i = 0$, the largest possible torque on the motor is $M_0 = \frac{k_M}{R_a} u_{max}$ and the largest possible angular velocity is $\Omega_0 = \frac{u_{max}}{k_E}$.
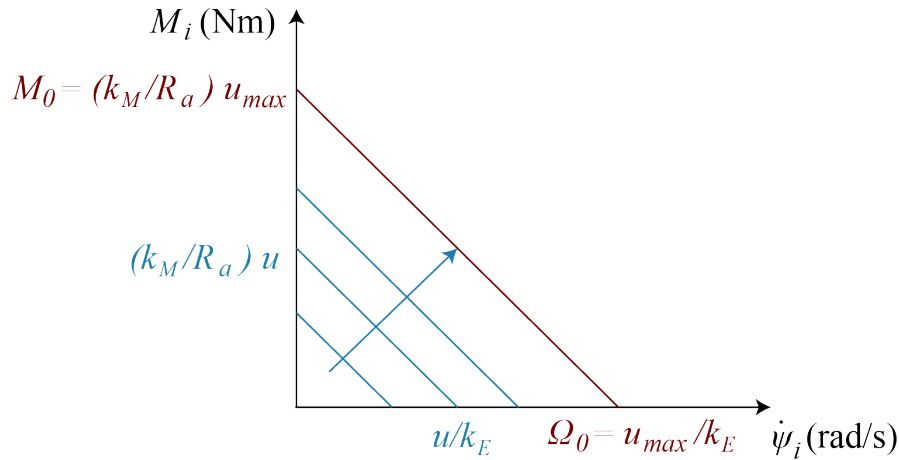

Figure 2. Approximate characteristic curves of the parallel DC motors: Adapted from Nóbrega, P. G., 1994

3 Two motors on connected foundations

The mathematical model to represent this case is shown in Fig. 3.

By calculating the kinetic and potential energy of the system, using the Euler-Lagrange equation, it is possible to find the equations of motion of the system.

$$(m + m_0)\ddot{x}_1 + c\dot{x}_1 + (k + k_f)x_1 = k_f x_2 - ma(\ddot{\psi}_1 sen\psi_1 + \dot{\psi}_1^2 cos\psi_1) \qquad (3)$$
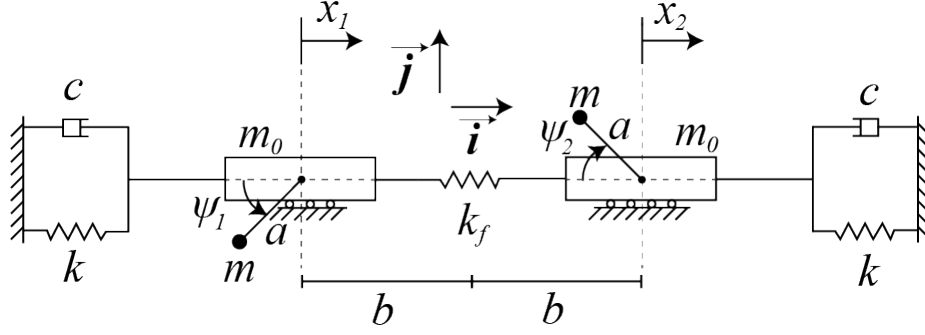
Figure 3. Mathematical model of two motors on connected foundations: Own authorship

$$(m + m_0)\ddot{x}_2 + c\dot{x}_2 + (k + k_f)x_2 = k_f x_1 - ma(\ddot{\psi}_2 sen\psi_2 + \dot{\psi}_2^2 cos\psi_2) \tag{4}$$

$$(ma^2 + I)\ddot{\psi}_i + ma\ddot{x}_i sen\psi_i = M_i \qquad \forall i \in \{1, 2\} \tag{5}$$

It is of interest to write the equations of motion using dimensionless variables. For this, new variables will be introduced in Table 1 and Table 2.

Table 1. New constants

Nomenclature	Name	calculation formula
u_{max}	Maximum voltage	Maximum voltage that the motor is subjected.
α	Proportion of eccentric masses	$m/(m_o + m)$
β	Proportion of elastic coefficients	$k_f/(k + k_f)$
γ	Dimensionless maximum torque	$\eta M_0/(ma^2\omega^2)$
δ	Proportion between resistance and inductance	$R_a/(L_a\omega)$
η	Proportion of the inertia	$ma^2/(ma^2 + I)$
ξ	Dimensionless damping	$0.5c\omega/(k + k_f)$
φ	Dimensionless maximum voltage	$u_{max}/k_E\omega$
ω	System frequency with stopped rotor	$\sqrt{(k + k_f)/(m_o + m)}$

Table 2. Dimensionless new variables

Nomenclature	Name	calculation formula
F_i	Percentage of torque supply	M_i/M_0
q_i	Dimensionless foundation displacement	x_i/a
v	percentage of voltage supply	u/u_{max}
τ	Dimensionless time	ωt

The derivative with respect to the dimensionless time is indicated by an apostrophe, for example, $\dot{q} = q'\omega$. From eq. (3), eq. (4) and eq. (5) with dimensionless variables, the following equations are obtained:

$$q_1'' = -\frac{2\xi q_1' + q_1 - \beta q_2 + \alpha(\gamma F_1 sen\psi_1 + \psi_1'^2 cos\psi_1)}{1 - \eta\alpha sen^2\psi_1} \tag{6}$$

$$q_2'' = -\frac{2\xi q_2' + q_2 - \beta q_1 + \alpha(\gamma F_2 sen\psi_2 + \psi_2'^2 cos\psi_2)}{1 - \eta\alpha sen^2\psi_2} \tag{7}$$

$$\psi_1'' = \frac{\gamma F_1 + \eta sen\psi_1[2\xi q_1' + q_1 - \beta q_2 + \alpha\psi_1'^2 cos\psi_1]}{1 - \eta\alpha sen^2\psi_1} \tag{8}$$

$$\psi_2'' = \frac{\gamma F_2 + \eta sen\psi_2[2\xi q_2' + q_2 - \beta q_1 + \alpha\psi_2'^2 cos\psi_2]}{1 - \eta\alpha sen^2\psi_2} \tag{9}$$

Using eq. (2), the dimensionless motor equation can be written as below.

$$F_i' = \delta(v - \frac{\psi_i'}{\varphi} - F_i) \qquad \forall i \in \{1, 2\}. \tag{10}$$

4   Numerical model

The computational code used for data collection was programmed in Python. The fourth order Runge-Kutta method was used to obtain the model results over time. To obtain the sections (planes) of the basins of attraction, the $(\psi_2 - \psi_1)$ x $(\psi_2' - \psi_1')$ plane was chosen at different voltages. This plane was divided into several square segments and, for each segment, the attractor to which the model converged was obtained. Specifically to obtain the sections of the basins of attraction, the electrical voltage was considered constant over time ($v(t) = 1$), in order that its increase does not influence the attractor.

5   Results and discussion

In this study it was identified that synchronizations occur for unbalanced rotors angle differences of zero and π radians. Synchronization occurs faster the higher is the voltage of the motors. Figure 4 and Fig. 5 show $\psi_1 - \psi_2$ over time until the system converges.
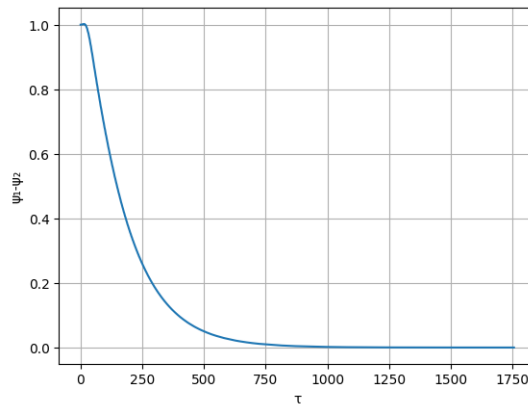

Figure 4. $\psi_2 - \psi_1$ x τ graphic for convergence where $\psi_2 - \psi_1 = 0$: Own authorship

To verify the change of the attractors with the increase of the voltage, the sections of the basins of attraction in the $(\psi_2 - \psi_1)$ x $(\psi_2' - \psi_1')$ planes with different φ (dimensionless voltages) were obtained. It was observed in Fig. 6, Fig. 7 and Fig. 8 that there is a gradual change of attractors between 0.66 and 0.74 ($6, 7$ V and $7, 5$ V), in addition to a change of attractors between 1.25 and 1.39 ($12, 7$ V and $14, 1$ V), observed in Fig. 9, Fig. 10 and Fig. 11.
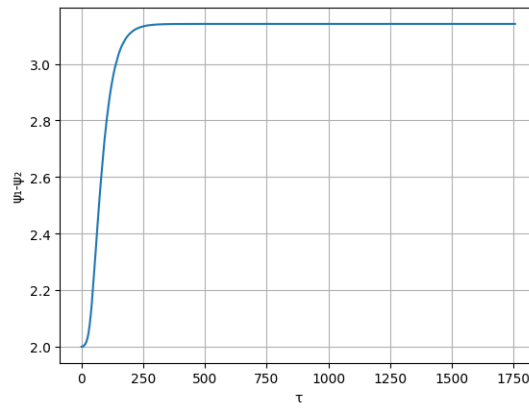
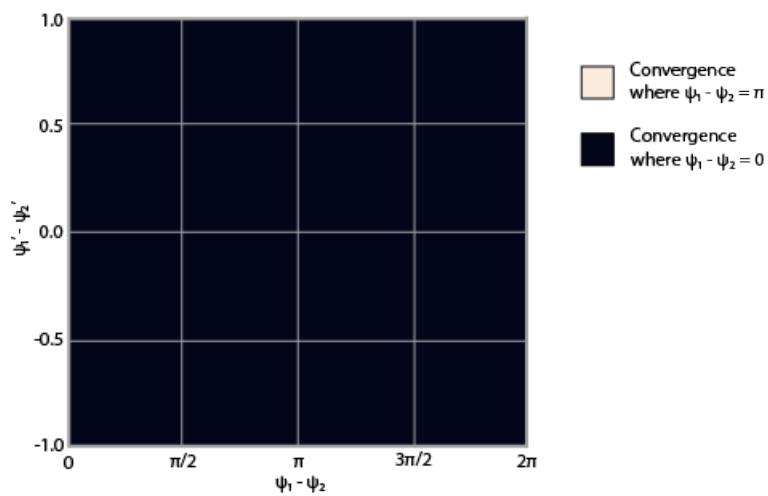Figure 5. $\psi_2 - \psi_1$ x τ graphic for convergence where $\psi_2 - \psi_1 = \pi$: Own authorship

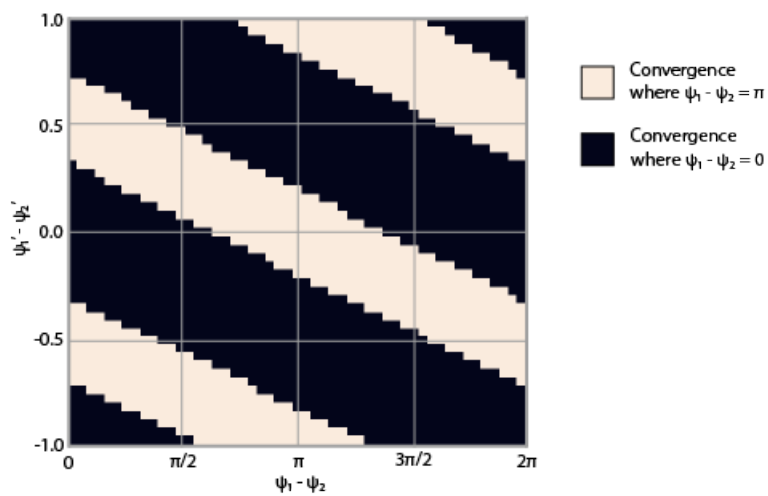Figure 6. Basin of attraction section when $\varphi = 0.66$: Own authorship

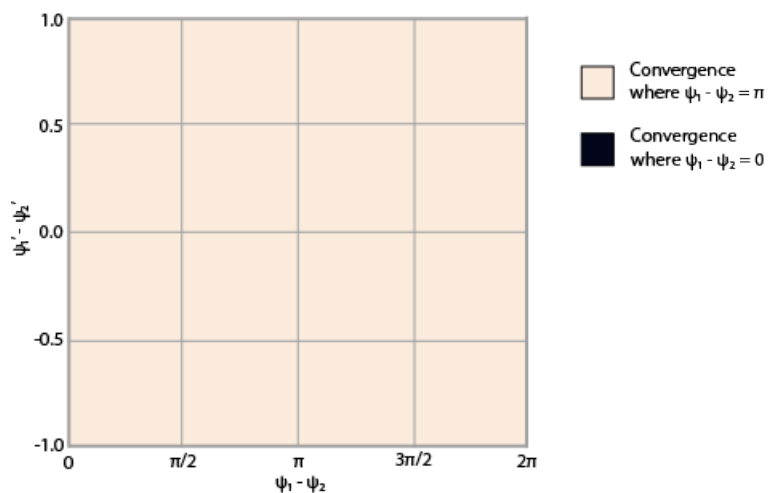Figure 7. Basin of attraction section when $\varphi = 0.70$: Own authorship

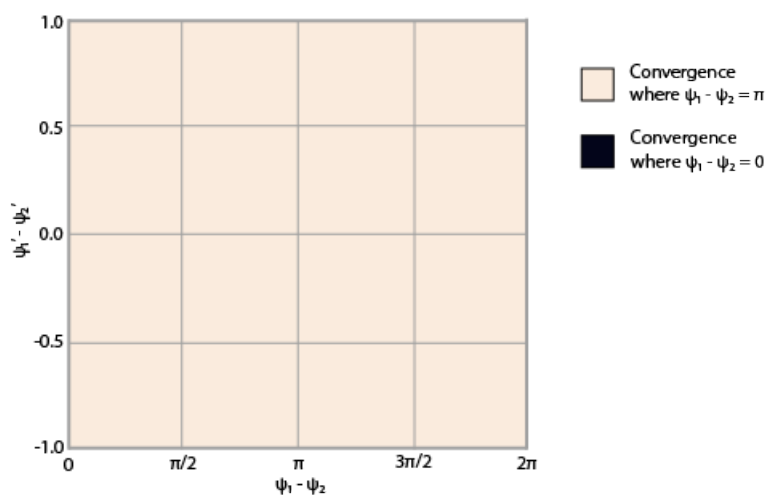Figure 8. Basin of attraction section when $\varphi = 0.74$: Own authorship

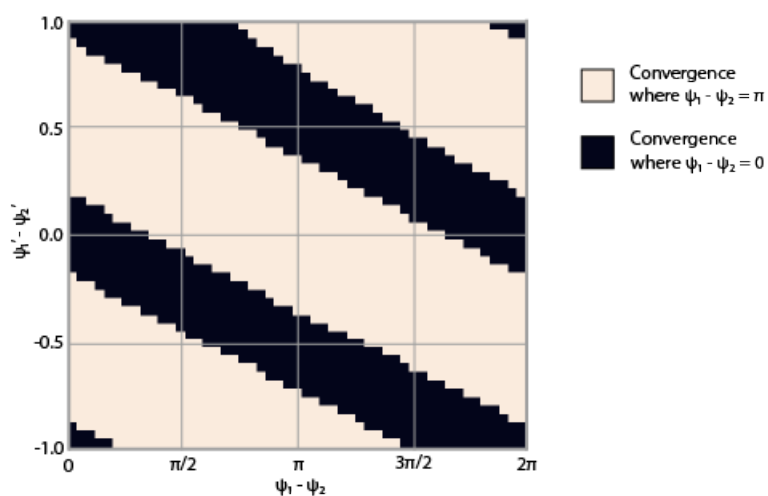Figure 9. Basin of attraction section when $\varphi = 1.25$: Own authorship

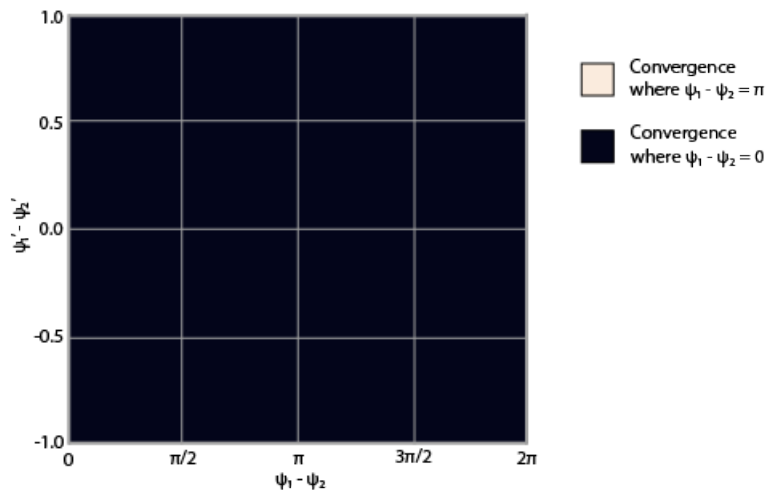Figure 10. Basin of attraction section when $\varphi = 1.32$: Own authorship

Figure 11. Basin of attraction section when $\varphi = 1.39$: Own authorship

6 Conclusions

The research fulfilled the objectives to study the case of motors on different foundations. It was seen that the type of convergence is related to the electrical voltages applied to the motors. The values of these factors that cause the change of attractors were studied.

Authorship statement. The authors hereby confirm that they are the sole liable persons responsible for the authorship of this work, and that all material that has been herein included as part of the present paper is either the property (and authorship) of the authors, or has the permission of the owners to be included here.

References

[1] P. G. Nóbrega. Auto-sincronização de motores não-ideais apoiados em estruturas elásticas. *São Paulo. Dissertação (Mestrado) - Escola Politécnica-Universidade de São Paulo*, 1994.

[2] V. O. Kononenko. *Vibrating systems with a limited power supply*. Iliffe, 1969.

[3] A. Sommerfeld. Über das wechselfeld und den wechselstromwiderstand von spulen und rollen. *Annalen der Physik*, vol. 320, n. 14, pp. 673–708, 1904.

[4] M. G. Say and E. O. Taylor. *Direct current machines*. Pitman, 1986.

[5] O. S. LOBOSCO and J. Dias. Seleção e aplicação de motores elétricos. *McGraw-Hill: Siemens, AS, São Paulo, 351p*, 1988.